

# The releasing behavior and in vitro osteoinductive evaluations of dexamethasone-loaded porous calcium phosphate cements

Azin Forouzandeh, Saeed Hesaraki\*, Ali Zamanian

*Nanotechnology and Advanced Materials Department, Materials & Energy Research Center, Alborz, Iran*

Received 11 February 2013; received in revised form 25 May 2013; accepted 28 June 2013

Available online 4 July 2013

## Abstract

In the present study, the effect of adding different concentrations of dexamethasone (DEX) on setting time, apatite formation and mechanical properties of micro/macroporous calcium phosphate cements (CPCs) was studied. The liberation of loaded DEX was evaluated over 0–840 h in simulated body fluid (SBF). Differentiation of mesenchymal stem cells on DEX-free and loaded CPCs were also compared by expression of bone marker proteins. The results showed that setting time decreased by adding DEX to CPCs whereas mechanical strength and conversion rate of cement reactants into apatite phase. A sustained release of DEX was observed from the loaded CPCs in which the rate of DEX release increased by introducing macroporosity and higher portion of loaded DEX.

Osteogenic differentiation of MSCs on DEX-loaded CPCs was confirmed by elevated gene expressions of bone markers such as alkaline phosphatase, osteopontin and osteocalcin. Overall, the results reveal that DEX-loaded CPCs may be potentially osteoinductive material with enhanced biological functions but more in vivo evaluations are required to prove this suggestion.

© 2013 Elsevier Ltd and Techna Group S.r.l. All rights reserved.

**Keywords:** Calcium phosphate(s); Bone cement; Drug release; Dexamethasone

## 1. Introduction

Calcium phosphate cements (CPCs) are promising alternatives for bone defect treatments because of their injectability, low temperature self-setting reactions and higher bioresorbability with respect to other bone substitutes [1–3]. CPCs can be easily molded into bone defects having irregular geometric shape and be hardened after several minutes. In order to improve in vivo resorption rate of CPCs, macroporosity has been introduced into them by using a variety of strategies such as salt leaching, phase separation, bubble entraining, freeze-drying, and gas foaming [4–7]. According to International Union of Pure and Applied Chemistry (IUPAC) definition the pores with a diameter less than 2 nm are called micropores and pores with a diameter larger than 50 nm are known as macropores [8]. However in tissue engineering area, macroporous materials are referred to scaffolds having pore diameters larger

than 50  $\mu\text{m}$  (at least) and materials with pore size of 1–10  $\mu\text{m}$  are called microporous. These macropores provide possibility of cell and tissue penetration within the bulk of cement and facilitate active resorption mechanism [9].

CPCs in micro- or macroporous forms are also potential to be loaded by different drugs and inorganic ions to treat bone diseases such as osteomyelitis or enhance rate of bone healing process as well as quality of regenerated bone [10–12]. For example, incorporation of Si and Zn ions into CPCs have been proved to enhance rate of bone healing process through stimulating effects on osteoblasts proliferation and regulating enzymatic reactions of these cells [13,14]. Using the ion-doped CPCs would result in formation of remodeled bone with mature structure (high quality) [15]. The prolonged liberation of several drugs and biomolecules from CPC matrices have been reported while biofunctionality of the liberated agent was even maintained [16]. However, the most problem of CPCs is lack of osteoinductivity. Osteoinduction is the process by which osteogenesis is induced. It is a phenomenon regularly seen in any type of bone healing process. Osteoinduction

\*Corresponding author. Tel.: +98 263 620 4131 4; fax: +98 261 620 1888.

E-mail address: [S-hesaraki@merc.ac.ir](mailto:S-hesaraki@merc.ac.ir) (S. Hesaraki).

Table 1

Compositions of CPCs according to concentration of SDS and DEX in the liquid phase.

[SDS] in CPC liquid (mM)	Concentration of DEX in the CPC liquid (nM)			
	0	10	50	100
0	s0-DEX0	s0-DEX10	s0-DEX50	s0-DEX100
100	s100-DEX0	s100-DEX10	s100-DEX50	s100-DEX100

implies the recruitment of immature cells and the stimulation of these cells to develop into preosteoblasts [17].

Many studies attempted to produce osteoinductive CPCs by incorporating bone morphogenic proteins (BMPs) and growth factors though these materials have a very high price [18,19].

Currently, osteogenic supplement as a mixture of ascorbic acid,  $\beta$ -glycerophosphate and dexamethasone was added to CPCs to produce an osteoinductive material [20]. Osteogenic differentiation of mesenchymal stem cells (MSCs) on these cements was confirmed by gene expressions of some bone marker proteins. However, the role of these reagents on basic properties of CPCs (e.g. setting time, apatite formation reactions, injectability and mechanical properties) have not been thoroughly discussed. Moreover, since a mixture of ascorbic acid,  $\beta$ -glycerophosphate and dexamethasone (DEX) was added to CPCs, the effect of each one on the basic properties and hydraulic reactions of CPCs is not clear.

DEX is a family of glucocorticoids with inhibitory effects on inflammations [21]. It has been reported that DEX molecules play important roles on regulation of genes and cellular reactions which are responsible for the growth and division of cells. The osteogenic induction of mesenchymal stem cells by DEX molecules either alone or in combination with ascorbate-2-phosphate has been reported previously [22,23].

CPCs are bone regenerative materials with inorganic compositional groups similar to bone mineral. The bone remodeling process at the presence of CPCs is conducted by known processes addressed by some authors [24]. Since CPCs are osteoconductive materials, the osteoblastic cells are encouraged to attach on the surface and even bulk (in the case of macroporous forms) of these materials, proliferate, do enzymatic activities and produce extra cellular matrix and all of these happenings would result in bone remodeling. Incorporation of DEX into CPCs and its release into the cells medium would offer a more efficient material in terms of osteogenic induction. Thus, in the present study, different concentrations of DEX (as the most important component of osteogenic agents) were added to micro and macroporous CPCs and the physical, mechanical and in vitro phase conversion behaviors of the obtained cements were investigated. The liberation of DEX from CPCs into a physiological solution was also studied. Moreover, osteogenic differentiation of rat-derived MSCs cultured on tops of different cement samples was evaluated. In this paper, the terms microporous CPC and macroporous CPC refer to cements without and with SDS, respectively.

## 2. Materials and methods

### 2.1. Preparation of DEX-loaded CPCs

Tetracalcium phosphate (TTCP) powder was synthesized at 1500 °C for 6 h by mixing 1 mol of dicalcium phosphate anhydride and 1 mol of calcium carbonate (both from Merck, Germany) [25]. It was milled to reach a powder with average particle size of 10  $\mu$ m. The powder phase of CPC was a mixture of 73 wt% TTCP and 27 wt% dicalcium phosphate anhydrous (DCPA). The liquid phase of CPC was a solution of 3 wt%  $\text{NaH}_2\text{PO}_4$ . Sodium dodecylsulphate (SDS) and dexamethasone (DEX) were also purchased from Sigma Company and introduced into cement liquid according to Table 1, as air bubble-entraining agent for producing macroporosity and DEX-loaded cement, respectively.

To fabricate CPC paste, the powder (*P*) was added to the liquid (*L*) phase (at a *P/L* ratio of 3 g/mL) and then mixed for 2 min until a homogenized paste was achieved.

### 2.2. Characterization of CPCs

The influence of SDS and DEX on the physical/physico-chemical properties of the CPCs was determined by characterizing initial setting time, compressive strength, injectability, porosity, and rate of apatite formation. The release behavior of DEX from the cements into simulated body fluid (SBF) solution was studied as well as osteogenic gene expression of rat-derived mesenchymal stem cells cultured on them.

The initial setting time (Ist) was recorded by a Gillmore needle in accordance with the ASTM C266-99-A standard. Ist is the time that a light needle (113.4 g, 2.13 mm in diameter) does not form a visible print onto the surface of the specimen.

To measure compressive strength (CS), CPC paste was prepared by mixing powder to liquid at *P/L* = 3 g/mL. Then, a cylindrical sample with a diameter of 6 mm and a height of 12 mm was shaped through molding paste into a Teflon mold. After setting, the specimen was removed from the mold, immersed in 50 mL of SBF solution prepared according to Kokubo's specification [26]. The compressive strength of wet specimen soaked in SBF for 1, 7 and 14 days was measured using a static mechanical testing device (STM 120, Santam Co.) at a crosshead speed of 1 mm/min.

For the injectability (*I*) measurements, eight grams of CPC paste was transferred into a 10 mL syringe (internal tip diameter of 800  $\mu$ m) and extruded by a compressive load vertically mounted on top of the plunger (STM 120, Santam Co.).

The crosshead speed of 15 mm/min was applied and the force–displacement curve was obtained. In this study, the syringe displacement and then volume of extruded paste at constant load of 100 N were measured and index of injectability was calculated as follows:

$$I(\%) = 100(\text{volume of extruded cement})/(\text{initial volume of the paste}) \quad (1)$$

For density and porosity measurements, five specimens were prepared for each cement composition similar to that of CS test. The bulk density ( $d_b$ ) was obtained from the following expression:

$$d_b = M_{CPC}/V_{CPC} \quad (2)$$

where  $M_{CPC}$  is mass of specimen and  $V_{CPC}$  is its volume. Total porosity ( $P_{total}$ ) measurements were performed on incubated dried specimens as follows:

$$P_{total} = 100(1 - (d_b/d_p)) \quad (3)$$

where  $d_p$  is powder density of CPC specimen obtained from pycnometry measurements. Macroporosity ( $P_{ma}$ ) was also determined by

$$P_{ma} = 100(1 - (d_b/d_0)) \quad (4)$$

where  $d_0$  is bulk density of dried samples without any additive. Finally, microporosity  $P_{mi}$  was obtained from the following equation:

$$P_{mi} = P_{total} - P_{ma} \quad (5)$$

The phase composition of specimens was determined by an X-ray diffractometer device (Philips PW 3710 with Cu-K $\alpha$  radiation). The XRD experiments were performed on cement powders and those specimens soaked in SBF solution for 1, 7 and 14 days (37 °C). In brief, after each evaluating period, the specimen was washed with distilled water, dried at room temperature, grounded to fine powder, weighted and then characterized. Data were acquired from 10 to 60° 2 $\theta$  with a scan rate of 0.02, 2 $\theta$ /s. Five specimens of each composition were tested.

To obtain the effect of added SDS and DEX on crystallinity of CPCs, after 14 days of soaking, diffraction peak of (002) plane (corresponding to 2 $\theta$  = 25.9°) was recorded a minimum of five times at 0.05 2 $\theta$ /min. The peak width at half of maximum height was measured and corrected for instrumental broadening by Warren's method: [27,28]

$$\beta^2 - b^2 = B^2 \quad (6)$$

where  $b$  is instrumental broadening,  $B$  is corrected peak width and  $\beta$  is peak width at half of maximum intensity.

Morphological observations of CPCs were performed by using a scanning electron microscope (Stereoscan S 360) worked at accelerating voltage of 15 kV. Because of poor electrical conductivity of CPCs, the specimen was coated with a thin layer of gold before testing.

### 2.3. Drug release study

The release behavior of DEX was determined over 840 h in SBF solution. A weighed cylindrical specimen was immersed in a dark-glassy bottle containing 50 mL of the SBF solution and then the bottles were completely sealed to avoid inclusion of external things. The container was placed over an orbital shaker and the set up was transferred into an incubator. The release test was conducted under rotational situation (20 rpm) and in 5% CO<sub>2</sub>/95% air atmosphere at 37 °C to prevent bacteria proliferation in the SBF solution. After defined time intervals (7, 16, 24, 144, 264, 408, 504, 672 and 840 h), the solutions were analyzed by UV–visible spectroscopy (UV/VIS spectrometer Lambda 25, Perkinelmer US) at 202 nm. The concentration of the released DEX was determined using a calibration curve in which UV absorption intensity was plotted against known concentrations of DEX solutions. It should be noted that the SBF solution was refreshed every 24 and the cumulative concentration of DEX was plotted against time.

To realize the mechanisms of DEX release, the power law [29] (Eq. 7) and Weibull [30] (Eq. 8) equations were fitted on experimental data

$$M_t/M_0 = kt^n \quad (7)$$

$$M_t/M_0 = 1 - \exp(-(t/\tau)^d) \quad (8)$$

where  $M_t$  is cumulative amount of released drug at time  $t$ ,  $M_0$  is initial amount of loaded drug,  $k$  and  $\tau$  are kinetic constants,  $n$  is release exponent and  $d$  is Weibull constant.

### 2.4. Proliferation and osteogenesis differentiation of mesenchymal stem cells on DEX-free and DEX-loaded CPCs

Bone marrow MSCs were isolated from tibia bone shaft of the Wistar rat. The medium consisted of Dulbecco modified Eagle medium supplemented with 15% fetal bovine serum and 100 g/mL penicillin–streptomycin. The bone marrow suspensions were cultured in polystyrene 6-well culture dishes. Nonadherent cells were removed from the cultures after 4 days by a series of PBS washes and subsequent medium changes. Adherent cells were expanded as monolayer cultures. The confluent cells were dissociated with trypsin and sub-cultured in new 6-well culture dishes at a plating density of  $6 \times 10^4$  cells/dish. These handlings were repeated several times until sufficient numbers of cells were produced.

Cells from 3rd passage were seeded at density of  $2 \times 10^4$  onto disc-shaped samples (s0-DEX0, s0-DEX50 and s100-DEX50) (6 mm in diameter and 3 mm in height) in several multi-well dishes. The cell-loaded samples were incubated in a non-differentiation-medium of DMEM supplemented with 15% FBS for 1–14 days.

The proliferation of the osteoblastic cells was determined using the MTT (3-[4,5-dimethylthiazol-2-yl]-2,5-diphenyl-2H-tetrazolium bromide) assay. For this purpose, at the end of each evaluating period, the medium was removed and 2 ml of MTT solution was added to each well. Following incubation at 37 °C for 4 h in a fully humidified atmosphere at 5% CO<sub>2</sub> in

air, MTT was taken up by active cells and reduced in the mitochondria to insoluble purple formazon granules. Subsequently, the medium was discarded and the precipitated formazon was dissolved in dimethylsulfoxide, DMSO, (150 ml/well), and optical density of the solution was read using a microplate spectrophotometer (BIO-TEK Elx 800, Highland park, USA) at a wavelength of 570 nm.

The morphology of MSCs attached onto the surfaces of samples was observed by SEM instrument. For this purpose, the cells were cultured onto the discs which were rinsed with phosphate buffered saline (PBS) twice and then the cells were fixed with 500 mL/well of 3% glutaraldehyde solution (diluted from 50% glutaraldehyde solution with PBS). After 30 min, they were rinsed again and kept in PBS at 4 °C. The specimens were then fixed with 1% osmium tetroxide (Polyscience, Warrington, PA, USA). After cell fixation, the specimens were dehydrated in ethanol solutions of varying concentrations of 30, 50, 70, 90, and 100% for about 20 min at each concentration. The specimens were then dried in air, coated with thin layer of gold and analyzed by SEM device (Streoscan S 360, Cambridge).

The total RNA of cells was isolated at 7 and 14 days after incubation by high pure isolation RNA kit (Roche Diagnostics, Germany). The concentration of RNA was found out using a Nanodrop ND-1000 spectrophotometer at 260 nm. The samples were then reversed-transcribed into cDNA using an iScript cDNA synthesis kit (BIO-RAD). Real-time PCR was started on an ABI Prism 7500 sequence detection system (ABI, Fostercity, CA) using a cDNA product pattern, specific primers,

and iQSYBR Green supermix (BIO-RAD). Primer sequences employed for Runx2, osteopontin, osteocalcin, ALP and glyceraldehyde 3-phosphatedehydrogenase (GAPDH) are shown in Table 2. They were prepared from invitrogen and used to assess gene expression [31]. The relative quantification of genes expression was made using the 2- $\Delta\Delta C_t$  method [32] by normalizing with GAPDH gene as an endogenous control.  $\Delta\Delta C_t$  was calculated from

$$(C_t, \text{sample} - C_t, \text{control})_{\text{target gene}} - (C_t, \text{sample} - C_t, \text{control})_{\text{GAPDH}} \quad (9)$$

### 2.5. Calculations and statistical analysis

Data were processed using Microsoft Excel 2010 software and the results were presented as mean  $\pm$  standard deviation of at least 4 experiments. Significance between the mean values was calculated using standard software program (SPSS GmbH, Munich, Germany) and the  $p \leq 0.05$  was considered significant.

## 3. Results and discussion

### 3.1. Physical properties and phase composition of CPCs

The mean particle size (d50) of TTCP and DCPD were 12 and 5  $\mu\text{m}$ , respectively.

The initial setting time, compressive strength and injectability index of various CPCs have been shown in Table 3.

The setting time is affected by adding SDS molecules to the cement composition. The CPC pastes without SDS have a setting time of about 25 min. The initial setting time increases by about 28% when SDS molecule is used. However, adverse result is obtained by using DEX. The initial setting time of all CPCs (with and without SDS) significantly decreases by incorporating DEX into the CPC composition. For example, addition of 10 nM DEX to s0-DEX0 cement causes to a reduction of setting time by about 20%. Formation of apatite phase from the hydraulic reaction of TTCP and DCPA is a dissolution–precipitation phenomenon which has been described in literatures [33]. Entanglement of the early-formed apatite crystals is responsible for cement hardening and provides mechanical strength. Decrease in setting time of CPCs by introducing DEX molecules is probably due to the

Table 2  
Sequences of primers used in real-time PCR analysis.

Genes	Sequence
Osteocalcin	For: 5'-TGT GAG CTC AAT CCG GAC TGT Rev: 5'-CCG ATA GGC CTC CTG AAG C
Osteopontin	For: 5'-ATG AGA TTG GCA GTG ATT Rev: 5'-TTC AAT CAG AAA CCT GGA A
Alkaline phosphatase (ALP)	For: 5'-ACC ATT CCC ACG TCT TCA CAT TT Rev: 5'-AGA CAT TCT CTC GTT CAC CGC C
Runx2	For: 5'-AGA TGA TGA CAC TGC CAC CTC TG Rev: 5'-GGG ATG AAA TGC TTG GGA ACT
GAPDH	For: 5'-AAC AGC GAC ACC CAC TCC TC Rev: 5'-CAT ACC AGG AAA TGA GCT TGA CAA

Table 3  
Initial setting time, compressive strength and injectability of CPCs with or without SDS and DEX additives.

	Ist (min)	CS of 1 day-soaked CPCs (MPa)	CS of 7 days-soaked CPCs (MPa)	CS of 14-days soaked CPCs (MPa)	I (%)
s0-DEX0	25.1 $\pm$ 1.2	10.7 $\pm$ 1.2	10.9 $\pm$ 2.1	11.3 $\pm$ 2.2	50 $\pm$ 1
s0-DEX10	21.5 $\pm$ 0.8	11.1 $\pm$ 1.7	15.2 $\pm$ 3.4	11.5 $\pm$ 1.5	49 $\pm$ 2
s0-DEX50	20 $\pm$ 1.1	11.4 $\pm$ 2.8	20.9 $\pm$ 3.5	17.7 $\pm$ 2.4	47 $\pm$ 3
s0-DEX100	22.1 $\pm$ 1.0	12.5 $\pm$ 2.2	22.1 $\pm$ 3.0	18.8 $\pm$ 1.9	52 $\pm$ 2
s100-DEX0	32.4 $\pm$ 0.7	1.7 $\pm$ 0.9	8.9 $\pm$ 0.8	8.8 $\pm$ 1.3	58 $\pm$ 2
s100-DEX10	28.7 $\pm$ 1.2	2.0 $\pm$ 0.4	5.3 $\pm$ 1.7	5.7 $\pm$ 1.1	57 $\pm$ 3
s100-DEX50	24.8 $\pm$ 1.1	3.7 $\pm$ 0.7	8.8 $\pm$ 2.0	8.8 $\pm$ 3.0	57 $\pm$ 2
s100-DEX100	26.5 $\pm$ 0.9	2.4 $\pm$ 0.5	6.0 $\pm$ 1.7	7.4 $\pm$ 1.6	55 $\pm$ 3



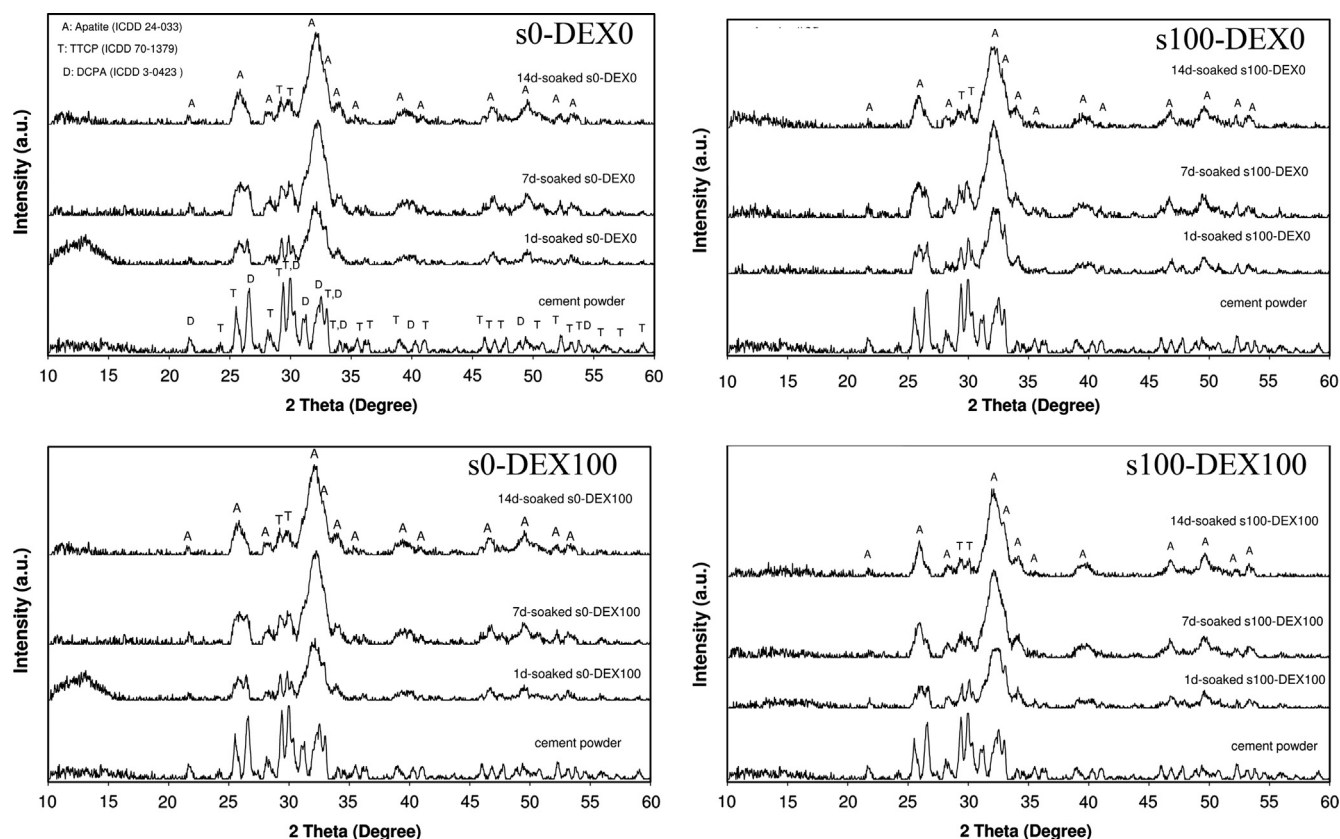


Fig. 1. The XRD patterns of macro- and microporous CPCs with different concentrations of DEX soaked in SBF solution for different periods.

formation of an organic–inorganic complex which was followed by reaction of DEX organic acid molecules with calcium phosphate base particles.

In terms of compressive strength, for all soaking times, the compressive strength of porous samples (cements containing SDS) is significantly lower than that of SDS-free ones. After 1 day of soaking, the compressive strength values of SDS-free CPCs with or without DEX are in the range of 10–12 MPa and the differences are not statistically significant. For s0-DEX0 and s0-DEX10, the compressive strength values in all soaking periods are comparable. However, in CPCs containing 50 and 100 nm DEX, the compressive strength values significantly improves after soaking for 7 and 14 days.

The injectability of microporous cements (with or without DEX) comes in the range of 47–52% and the differences between the average values are not statistically significant. Adding SDS to the cement composition leads to partial improvement of cement injectability. Overall, the cements do not exhibit good injectability (lower than 70%) and solid–liquid phase separation occurred during the injection process. It can be resulted from the relatively high powder to liquid ratio of the cements.

Fig. 1 shows the XRD diagrams of different CPCs soaked in SBF solution for different times. The pattern of cement powder is also shown for comparison. In all samples, after 1 day soaking, considerable amount of reactants (TTCP and DCPA) have been converted to apatite and it is the predominant phase. As time soaking goes on, peak intensity of apatite phase

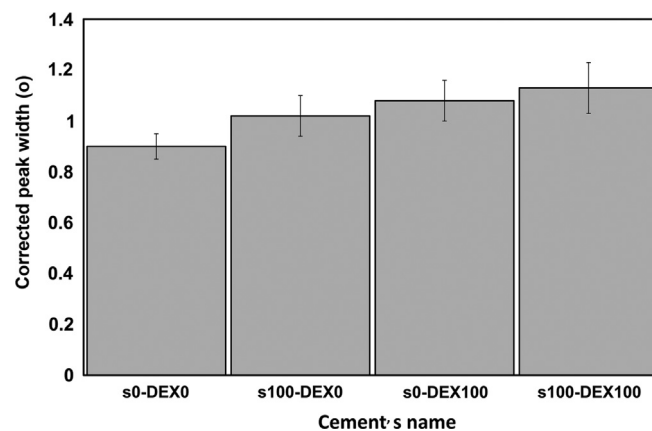


Fig. 2. Index of apatite peak broadening for different CPCs soaked in SBF solution for 14 days.

increases though small amount of TTCP has been still remained after 14 days. It should be taken into consideration that the presence of both SDS and DEX molecules did not affect the rate of TTCP and DCPA conversion into apatite product. The appearance of broad diffraction peaks reflects the poor crystallinity and fine crystallite size of the produced apatite phase.

Fig. 2 compares the corrected peak width value of CPCs soaked in SBF solution for 14 days. It is well known that the peak width inversely correlates with crystallinity (i.e. the smaller peak width, the larger and/or less strained crystals).

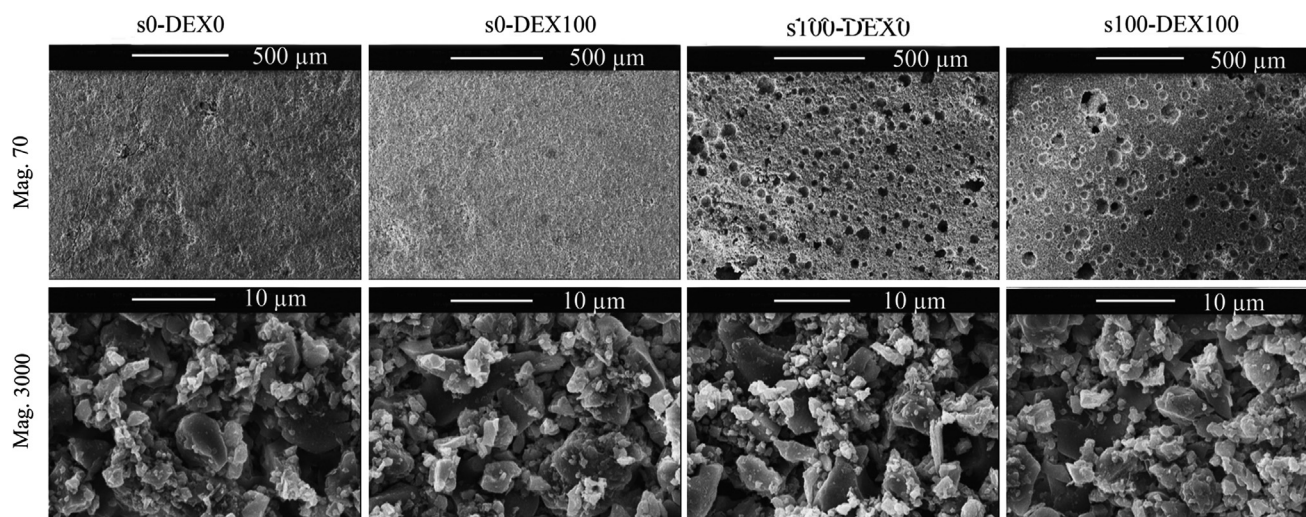


Fig. 3. The SEM images of CPCs before soaking in SBF solution taken at different magnifications.

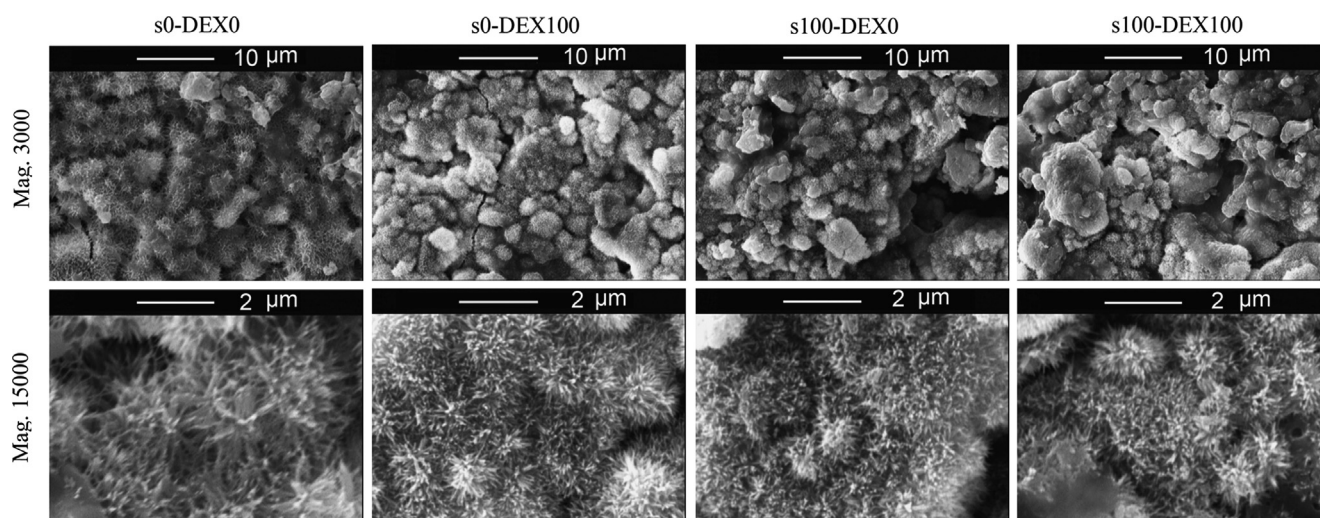


Fig. 4. Morphology of macro- and microporous CPCs containing different amounts of DEX after soaking in SBF solution for 14 days.

It is shown that the crystallinity significantly decreases (peak width increases) by adding SDS to CPC and further reduction is achieved by introducing DEX molecules.

Fig. 3 shows the morphology of CPCs before soaking in SBF solution, at two different magnifications. The low magnification shows that the presence of SDS molecules leads to creation of spherical macropores with pore diameter of 50–150  $\mu\text{m}$ . At higher magnification, irregular particles of TTCP and DCPA are observed that produced a microporous (1–10  $\mu\text{m}$ ) matrix.

Fig. 4 illustrates the surface morphology of CPCs after soaking in SBF solution for 14 days. The upper images show spherical particles, each one comprised of many needle like crystals. As shown in higher magnifications (lower images), the crystals have a tight entanglement to each other. It seems that the size and roughness of apatite crystals produced in SDS- and DEX-containing CPCs is lower than those produced in s0-DEX0. These results confirm the XRD peak width data shown in Fig. 2 and are in agreement with those of Sarda et al. [7] who prepared porous CPCs using SDS molecules.

In addition to macroporosity, the numbers of entangled crystals play important role in mechanical strength. For a constant volume of apatite crystals, the numbers of them will decrease if the size of them increases. It can explain, the higher compressive strength of the soaked SDS-free DEX-loaded cements, s0-DEX50 and s0-DEX100, compared to s0-DEX0 and s0-DEX10 (Table 3).

Conversion of cement reactants into apatite phase continues during the soaking procedure. Although the presence of SDS and liberated DEX molecules in the SBF medium did not affect the rate of apatite formation, the results of crystallinity and SEM images suggest that these molecules can be adsorbed on the surfaces of calcium phosphate particles and even apatite nuclei and retarded growth of these crystals. It should be taken into account that DEX is a carboxylic acid with hydrophobic nature (Fig. 5) and there are some reports that addressed the preventing effect of carboxylic acid molecules on apatite crystal growth through adsorption onto their surfaces [34].

Table 4 gives some information about density and porosity of CPCs with or without DEX. SDS-free samples have about 35–39% microporosity and the differences between the porosity values of DEX-containing samples and DEX-free ones are not statistically significant. The results reveal that the addition of SDS molecules to CPCs could introduce about 13–16% macroporosity in the cement structure and hence reduces the volume of micropores. The mechanism of pore formation using SDS molecules has been well discussed in literatures [7]. The SDS molecules trap air bubbles entered into cement paste during stirring and make them stabilized by interacting with calcium cations. The macropores are responsible for weak mechanical strength of SDS-containing CPCs.

### 3.2. DEX release

DEX is a synthetic glucocorticoid that supports the osteogenic differentiation of stem cells in vitro [35]. Thus, it was incorporated into CPCs to yield an osteoinductive material. DEX release was studied by the UV–visible absorption technique. Fig. 6 shows typical UV absorption bands of the SBF solution contained s0-DEX50 for various times. The adsorption peaks at 202 nm relate to DEX. The peak intensities correlate with concentration of DEX released from the CPC into the solution. As observed in this figure, for most soaking times, there is a direct relationship between the adsorption peak intensity of DEX and immersion time. However in some cases a diversity is observed. For example the peak intensity of DEX in the 11-days-soaked samples (264 h) is lower than that of 6-days soaked one (144 h). It can be related to the adsorption and desorption of DEX during the soaking period. In other words, the liberated DEX can return to the cement or adsorb on to the surface of CPC or the formed apatite crystals. Thus, at some intervals its concentration in the SBF solution

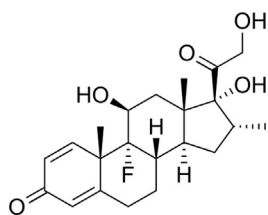


Fig. 5. Chemical structure of DEX molecules.

can decrease. Fig. 7 shows the cumulative concentration of DEX released from different CPCs as a function of time. The power law and Weibull equations fitted on the experimental data are also shown. All cements exhibit good potential for long term maintenance of DEX. The results determine that the rate of release increases when using SDS molecules and higher DEX dosage, because at defined intervals, differences in the concentrations of DEX loaded on different samples are

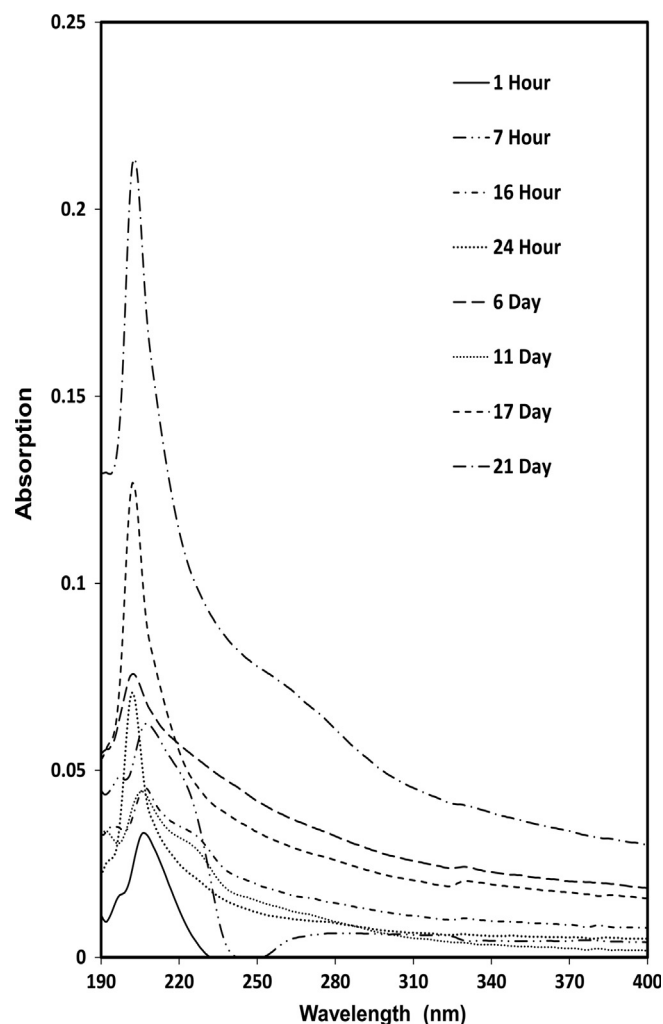


Fig. 6. Typical UV visible absorption spectra of SBF solution contained DEX-loaded CPCs for various periods.

Table 4  
Density and porosity information of CPCs with or without SDS and DEX additives.

CPC	$d_b$	$P_t$	$P_{ma}$	$P_{mi}$
s0-DEX0	$1.71 \pm 0.07$	$39.2 \pm 2.6$	0	$39.2 \pm 2.6$
s0-DEX10	$1.74 \pm 0.10$	$38.2 \pm 3.6$	0	$38.2 \pm 3.6$
s0-DEX50	$1.77 \pm 0.05$	$37.0 \pm 1.8$	0	$37.0 \pm 1.8$
s0-DEX100	$1.81 \pm 0.04$	$35.8 \pm 2.4$	0	$35.8 \pm 2.4$
s100-DEX0	$1.45 \pm 0.02$	$48.5 \pm 0.7$	$13.7 \pm 1.1$	$34.8 \pm 0.4$
s100-DEX10	$1.46 \pm 0.02$	$47.9 \pm 1.0$	$15.6 \pm 1.6$	$32.3 \pm 0.6$
s100-DEX50	$1.48 \pm 0.02$	$47.3 \pm 0.8$	$16.1 \pm 1.3$	$31.2 \pm 0.4$
s100-DEX100	$1.50 \pm 0.01$	$46.4 \pm 0.7$	$16.7 \pm 1.0$	$29.7 \pm 0.4$



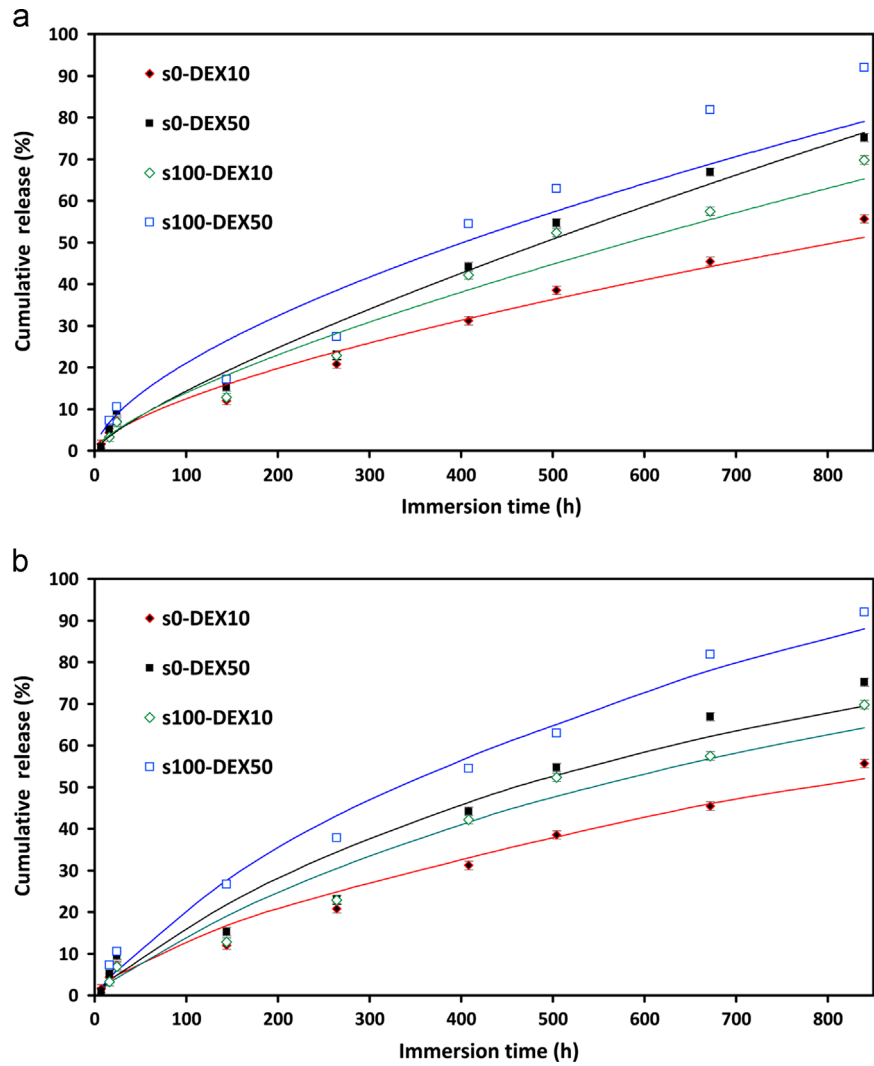


Fig. 7. Cumulative release of DEX from macro- and microporous CPCs along with power law (a) and Weibull and (b) equations fitted on experimental data.

Table 5  
Component of power law and Weibull equations fitted on experimental release data.

CPC	Power law			Weibull equation		
	$K$	$n$	$R^2$	$d$	$\tau$	$R^2$
s0-DEX10	$0.583 \pm 0.121$	$0.664 \pm 0.103$	0.967	$0.829 \pm 0.019$	$1473.8 \pm 125.2$	0.981
s0-DEX50	$0.381 \pm 0.152$	$0.787 \pm 0.031$	0.92	$0.893 \pm 0.026$	$694.4 \pm 35.6$	0.975
s100-DEX10	$0.487 \pm 0.161$	$0.717 \pm 0.025$	0.963	$0.900 \pm 0.019$	$814.0 \pm 55.8$	0.971
s100-DEX50	$1.197 \pm 0.230$	$0.622 \pm 0.029$	0.937	$0.928 \pm 0.039$	$487.9 \pm 64.3$	0.985

statistically significant ( $p < 0.05$ ). In other words, microporous cement (SDS-free CPCs) with the least DEX concentration exhibits minimum rate of release in which only 50% of the loaded DEX is released after 35 days. When macropores are produced in the cement structure, the release rate improves so that after 35 days, 90% of the loaded DEX is delivered. It is suggested that the presence of macropores can facilitate DEX transport through CPC matrix and consequently increase release rate. Table 5 represents the fit parameters of power law and Weibull's equation with each corresponding correlation

coefficient. Overall, liberation of DEX from all CPCs followed Weibull's equation much better than power law one. For both release exponent ( $n$ ) and Weibull constant ( $d$ ), the differences in values of different samples are not statistically significant but differences in the constant values ( $k$  and  $\tau$ ) are statistically significant. It discloses that there are the same DEX release mechanisms for all cements but the rate of liberation is different because " $k$ " and " $\tau$ " are dependents of physical and geometrical characteristics of the loaded matrix (such as specific surface area, porosity and tortosity) while " $n$ " and " $d$ " determine



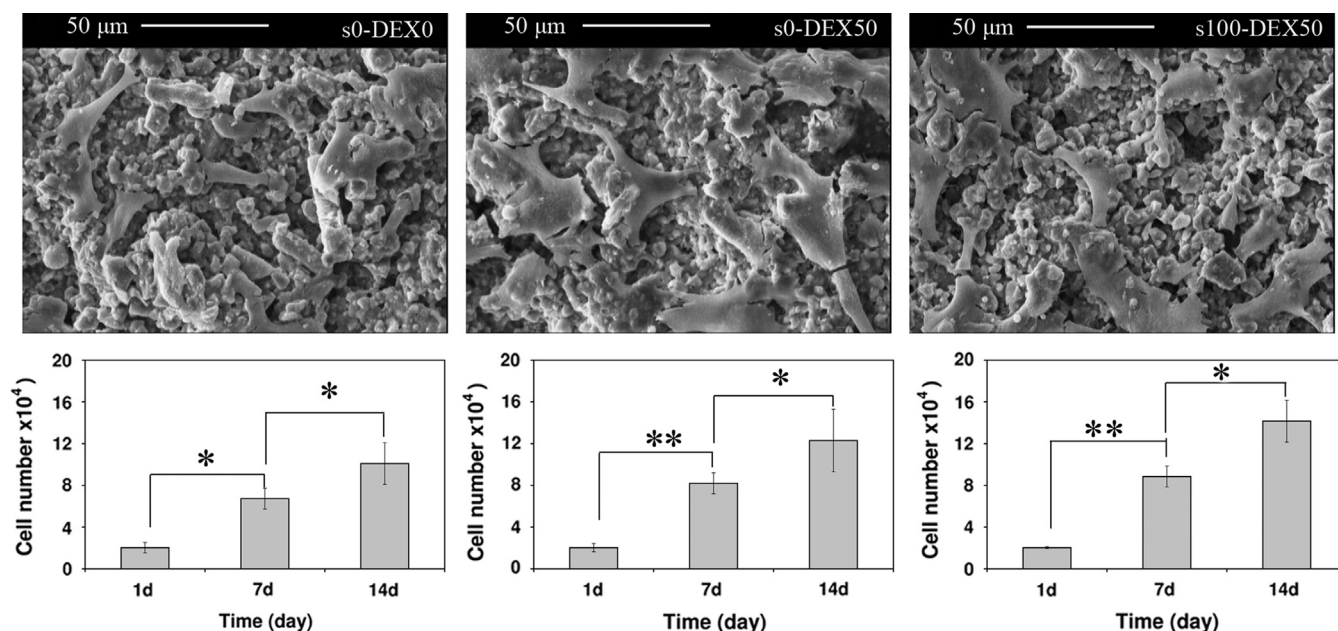


Fig. 8. The morphology of MSCs adhered on top of 1day-cultured s0-DEX0, s0-DEX50 and s100-DEX50 specimens along with numbers of viable cells at different periods.

release mechanism [36]. The presence of macropores can result in higher specific surface area, increasing  $k$  (or decreasing  $\tau$ ) value and hence fasten release process.

Since in DEX-loaded CPCs, the rate of drug release is much lower than the rate of cement resorption, this suggests that DEX release is a diffusion-controlled process [37].

Another important point which should be considered is better description of DEX release using Weibull's equation. Although power law gives relatively good regression with experimental data ( $R^2=0.92\text{--}0.96$ ), this model is just suitable for release description at short periods [38] and for the whole of release time, Weibull model gives better correlation coefficient (Table 5).

Sustained release of DEX from polymeric tissue engineering scaffolds (such as poly-lactic-glycolic acid and poly-lactic acid-collagen) and osteogenic differentiation of MSCs on these scaffolds have been reported elsewhere [22,39]. In this study, it was shown that CPCs are better alternatives for the release of DEX, because in contrast to polymeric scaffold in which high level of burst release ( $\sim 50\%$ ) was observed and about 90% of the loaded DEX was liberated after 22 days (528 h), CPCs liberated 30–50% of the loaded DEX after 500 h. In its porous forms, CPCs delivered about 90% of incorporated DEX after 840 h. In addition to poor water solubility of DEX, two other possible reasons are suggested for its slow release from CPCs: (i) interaction of organic acid molecules with calcium ions which leads to the formation of DEX–calcium phosphate complex. Because of the very slight concentration of DEX molecules (nanomolar), it is difficult to show these interactions using analytical methods. However these possible interactions (at the COOH terminal of organic acid molecules and Ca ions of the cement) have been proposed by other authors who studied release of drugs with R-COOH structure from calcium phosphate cements [40]. (ii) The change in the nature of loaded

matrix, i.e. conversion of the cement reactants into apatite phase. It may result in trapping DEX molecules within the apatite crystals.

### 3.3. Cell proliferation and gene expression

Fig. 8 illustrates morphology of cells adhered on the top of 1day-cultured s0-DEX0, s0-DEX50 and s100-DEX50 specimens along with numbers of viable cells at different periods. All cements which have microporous structure thoroughly supported cell attachment, because cells with polygonal morphologies and extended cytoplasmic membranes are observed over samples. The cells could proliferate on all samples, because the number of attached cells significantly increases with time. ( $p < 0.05$ ). However, it is observed that the rate of cell proliferation on DEX-containing CPCs is significantly ( $p < 0.05$ ) higher than that of s0-DEX0 at the similar periods. Biological activity of DEX loaded on CPCs was checked by determining osteogenic gene expression of rat-derived MSCs seeded on the samples in an osteogenic-free medium. The expression of Runx2 (osteogenic transcription factor), ALP (early differentiation gene), osteopontin and osteocalcin (extracellular matrix proteins of bone tissue) genes were determined by real-time PCR after 7 and 14 days. GAPDH expression was also used as control group. Fig. 9 shows the osteogenic gene expression of MSCs cultured on s0-DEX0, s0-DEX50 and s100-DEX50 specimens. These results reveal that in comparison to s0-DEX0, MSCs cultured on s0-DEX50 and s100-DEX50 demonstrate significantly higher degree of Runx2, ALP, osteopontin and osteocalcin genes expression after 7 and 14 days. In particular, after 7 days, the expression levels of Runx2, ALP, osteopontin and osteocalcin genes in MSCs on s0-DEX50 are respectively

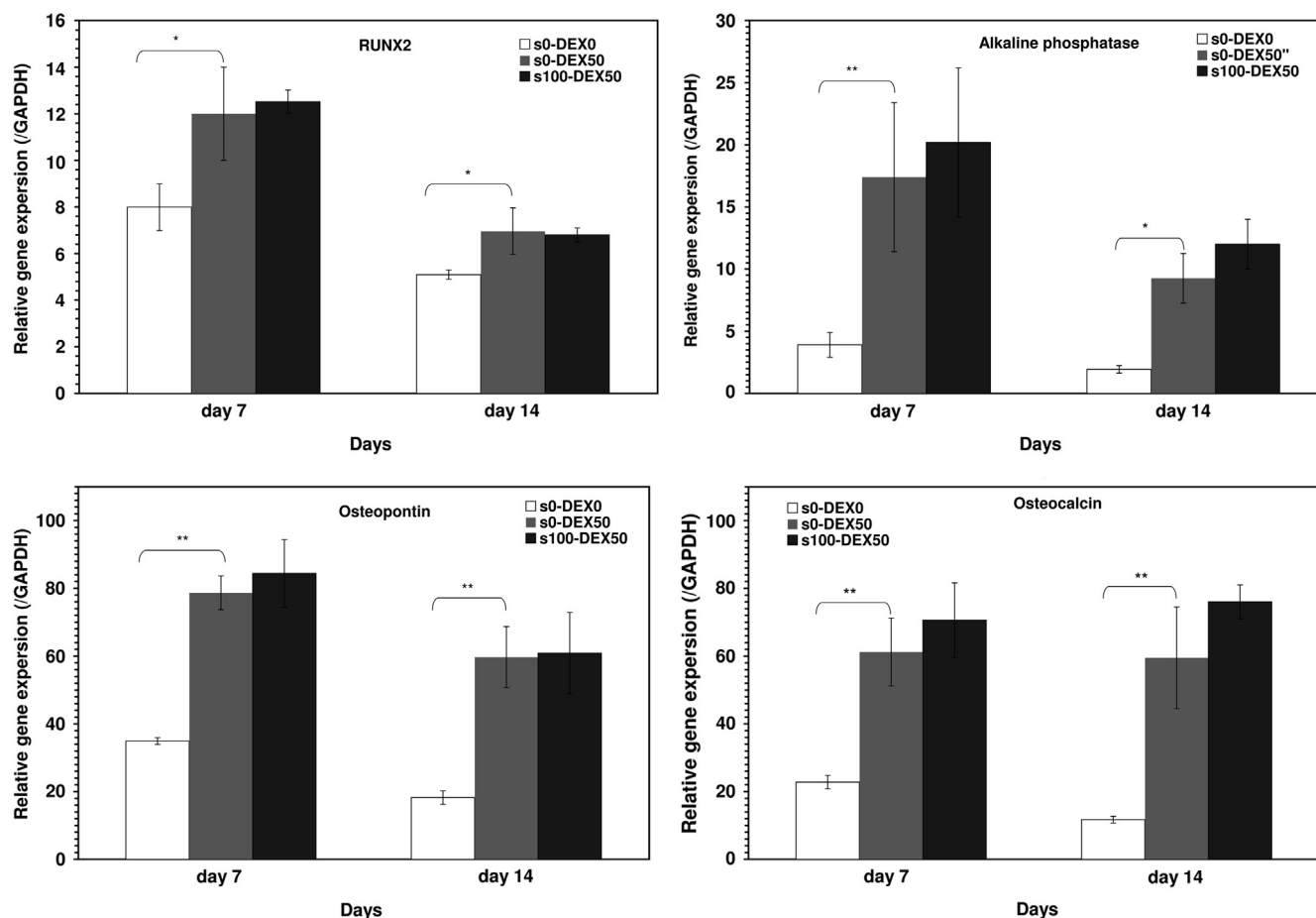


Fig. 9. The expression levels of bone marker proteins in MSCs cultured on s0-DEX0, s0-DEX50 and s100-DEX50 specimens.

1.5-, 4.7-, 2.2- and 2.8-folds of s0-DEX0. After 14 days, the levels of the genes expressed in MSCs on s0-DEX50 are respectively 1.4-, 4-, 3.3- and 6-folds of MSCs on s0-DEX0. Overall, the results demonstrate that DEX-added CPCs can preferentially adjust the expression of osteogenic-related genes.

Jaiswal et al. suggested that the effective concentration of DEX for the osteogenic differentiation of MSCs was in the range of 10 nM (40 ng/ml) to 100 nM and higher concentrations in culture medium would result in toxic effect [35]. According to the results, the concentration of released DEX falls in the therapeutic range which promotes osteogenic differentiation. Moreover, better osteogenic differentiation of MSCs on DEX-loaded CPCs compared to DEX-free samples determines that the possible interactions of DEX molecules and Ca ions of CPCs (which were previously addressed for the restricted release of DEX) did not influence on the bioavailability and activity of these molecules.

#### 4. Conclusions

From the results of this study, the following points can be concluded:

- DEX decreased setting time and crystallinity of the formed apatite phase in CPCs without any change in rate of cements hydraulic reactions.

- At preliminary stages of soaking, the mechanical strength of CPCs does not influence by DEX but higher compressive strength is achieved for DEX-loaded cements soaked for 7 and 14 days.
- CPCs are promising matrices for DEX loading, because they can liberate it during a relatively long period of time.
- The released DEX is biologically active, because it is able to differentiate mesenchymal stem cells to osteoblasts. It is found from well expression of bone marker proteins in MSCs cultured on DEX-loaded CPCs.

#### Acknowledgment

The authors acknowledge help of Dr. Hamid Nazarian and Mostafa Shahrezayee in cell studies.

#### References

- [1] S. Namdari, R. Rabinovich, J. Scolaro, K. Baldwin, M. Bhandari, S. Mehta, Absorbable and non-absorbable cement augmentation in fixation of intertrochanteric femur fractures: systematic review of the literature, *Archives of Orthopaedic and Trauma Surgery* 134 (2013) 487–494.
- [2] M. Bohner, U. Gbureck, J.E. Barralet, Technological issues for the development of more efficient calcium phosphate bone cements: a critical assessment, *Biomaterials* 26 (2005) 6423–6429.

- [3] G. Lewis, Viscoelastic properties of injectable bone cements for orthopaedic applications: state-of-the-art review, *Journal of Biomedical Materials Research B (Applied Biomaterials)* 98 (2011) 171–191.
- [4] H.H.K. Xu, J.B. Quinn, Calcium phosphate cements containing resorbable fibers for short-term reinforcement and macroporosity, *Biomaterials* 23 (2002) 193–202.
- [5] M. Markovic, S. Takagi, L.C. Chow, Formation of macropores in calcium phosphate cements through the use of mannitol crystals, *Key Engineering Materials* 122–1 (2000) 773–776.
- [6] J.E. Barralet, L. Grover, T. Gaunt, A.J. Wright, I.R. Gibson, Preparation of macroporous calcium phosphate cement tissue engineering scaffold, *Biomaterials* 23 (2002) 3063–3072.
- [7] S. Sarda, M. Nilsson, M. Balcells, E. Fernandez, Influence of surfactant molecules as air-entraining agent for bone cement macroporosity, *Journal of Biomedical Materials Research* 65A (2003) 215–221.
- [8] J.B. Condon, Surface Area and Porosity Determination by Physisorption Measurements and Theory, Elsevier, Amsterdam, Netherlands, 2–13.
- [9] R.P. Del Real, J.G.C. Wolke, M. Vallet-Regi, J.A. Jansen, A new method to produce macropores in calcium phosphate cements, *Biomaterials* 23 (2002) 3673–3680.
- [10] S. Bose, S. Tarafdar, Calcium phosphate ceramic systems in growth factor and drug delivery for bone tissue engineering: a review, *Acta Biomaterialia* 8 (2012) 1401–1421.
- [11] A.D. van Staden, L.M. Dicks, Calcium orthophosphate-based bone cements (CPCs): applications, antibiotic release and alternatives to antibiotics, *Journal of Applied Biomaterials and Functional Materials* 10 (2012) e2–e11.
- [12] F.C. van de Watering, J.D. Molkenboer-Kuennen, O.C. Boerman, J.J. van den Beucken, J.A. Jansen, Differential loading methods for BMP-2 within injectable calcium phosphate cement, *Journal of Controlled Release* 164 (2012) 283–290.
- [13] X. Li, Y. Sogo, A. Ito, H. Mutsuzaki, N. Ochiai, T. Kobayashi, S. Nakamura, K. Yamashita, R.Z. Legeros, The optimum zinc content in set calcium phosphate cement for promoting bone formation in vivo, *Materials Science and Engineering C: Materials for Biological Applications* 29 (2009) 969–975.
- [14] G. Mestres, C. Le Van, M.P. Ginebra, Silicon-stabilized  $\alpha$ -tricalcium phosphate and its use in a calcium phosphate cement: characterization and cell response, *Acta Biomaterialia* 8 (2012) 1169–1179.
- [15] C.L. Camiré, S.J. Saint-Jean, C. Mochales, P. Nevsten, J.S. Wang, L. Lidgren, I. McCarthy, M.P. Ginebra, Material characterization and in vivo behavior of silicon substituted alpha-tricalcium phosphate cement, *Journal of Biomedical Materials Research B Applied Biomaterials* 76 (2006) 424–431.
- [16] M.P. Ginebra, C. Canal, M. Espanol, D. Pastorino, E.B. Montufar, Calcium phosphate cements as drug delivery materials, *Advanced Drug Delivery Reviews* 64 (2012) 1090–1110.
- [17] O. Chan, M.J. Coathup, A. Nesbitt, C.Y. Ho, K.A. Hing, T. Buckland, C. Champion, G.W. Blunn, The effects of microporosity on osteoinduction of calcium phosphate bone graft substitute biomaterials, *Acta Biomaterialia* 8 (2012) 2788–2794.
- [18] W.J. Habraken, O.C. Boerman, J.G. Wolke, A.G. Mikos, J.A. Jansen, In vitro growth factor release from injectable calcium phosphate cements containing gelatin microspheres, *Journal of Biomedical Materials Research A* 91 (2009) 614–622.
- [19] M.D. Weir, H.H. Xu, Osteoblastic induction on calcium phosphate cement-chitosan constructs for bone tissue engineering, *Journal of Biomedical Materials Research A* 94 (2010) 223–233.
- [20] Y. Qu, Y. Yang, J. Li, Z. Chen, L. Li, K. Tang, Y. Man, Preliminary evaluation of a novel strong/osteoinductive calcium phosphate cement, *Journal of Biomaterials Applications* 26 (2011) 311–325.
- [21] M. Kawamura, K. Hatanaka, M. Saito, M. Ogino, T. Ono, K. Ogino, S. Matsuo, Y. Harada, Are the anti-inflammatory effects of dexamethasone responsible for inhibition of the induction of enzymes involved in prostanoind formation in rat carrageenin-induced pleurisy?, *European Journal of Pharmacology* 400 (2000) 127–135.
- [22] H. Kim, H.W. Kim, H. Suh, Sustained release of ascorbate-2-phosphate and dexamethasone from porous PLGA scaffolds for bone tissue engineering using mesenchymal stem cells, *Biomaterials* 24 (2003) 4671–4679.
- [23] H. Kim, H. Suh, S.A. Jo, H.W. Kim, J.M. Lee, E.H. Kim, Y. Reinwald, S.H. Park, B.H. Min, I. Jo, In vivo bone formation by human marrow stromal cells in biodegradable scaffolds that release dexamethasone and ascorbate-2-phosphate, *Biochemical and Biophysical Research Communications* 332 (2005) 1053–1060.
- [24] C.H. Tsai, R.M. Lin, C.P. Ju, J.H. Chern Lin, Bioresorption behavior of tetracalcium phosphate-derived calcium phosphate cement implanted in femur of rabbits, *Biomaterials* 29 (2008) 984–993.
- [25] S. Hesarak, F. Moztarzadeh, D. Sharifi, Formation of interconnected macropores in apatitic calcium phosphate bone cement with the use of an effervescent additive, *Journal of Biomedical Materials Research A* 83 (2007) 80–87.
- [26] T. Kokubo, H. Kushitani, S. Sakka, T. Kitsugi, T.J. Yamamuro, Solutions able to reproduce in vivo surface-structure changes in bioactive glass-ceramic A–W, *Journal of Biomedical Materials Research A* 24 (1990) 721–734.
- [27] B.D. Cullity, Elements of X-ray Diffraction, Addison-Wesley publishing Co, Massachusetts, 1978.
- [28] H.P. Kluy, L.E. Alexander, X-ray diffraction procedures for polycrystalline and amorphous materials, John Wiley & Sons, New York, 1974.
- [29] F. Tamimi, J. Torres, R. Bettini, F. Ruggera, C. Rueda, M. López-Ponce, E. Lopez-Cabarcos, Doxycycline sustained release from brushite cements for the treatment of periodontal diseases, *Journal of Biomedical Materials Research A* 85 (2008) 707–714.
- [30] U. Gbureck, E. Vorndran, F.A. Müller, J.E. Barralet, Low temperature direct 3D printed bioceramics and biocomposites as drug release matrices, *Journal of Controlled Release* 122 (2007) 173–180.
- [31] E.K. Yim, A.C. Wan, C. Le Visage, I.C. Liao, K.W. Leong, Proliferation and differentiation of human mesenchymal stem cell encapsulated in polyelectrolyte complexation fibrous scaffold, *Biomaterials* 27 (2006) 6111–6122.
- [32] K.J. Livak, T.D. Schmittgen, Analysis of relative gene expression data using realtime quantitative PCR and the  $2^{-\Delta\Delta CT}$  method, *Methods* 25 (2001) 402–408.
- [33] P.W. Brown, M. Fulmer, Kinetics of hydroxyapatite formation at low temperature, *Journal of the American Ceramic Society* 74 (1991) 934–940.
- [34] S. Hesarak, A. Zamanian, F. Moztarzadeh, The influence of the acidic component of the gas-foaming porogen used in preparing an injectable porous calcium phosphate cement on its properties: acetic acid versus citric acid, *Journal of Biomedical Materials Research B (Applied Biomaterials)* 86 (2008) 208–216.
- [35] N. Jaiswal, S.E. Haynesworth, A.I. Caplan, S.P. Bruder, Osteogenic differentiation of purified, culture-expanded human mesenchymal stem cells in vitro, *Journal of Cellular Biochemistry* 64 (1997) 295–312.
- [36] S. Hesarak, F. Moztarzadeh, N. Nezafati, Evaluation of a bioceramic-based nanocomposite material for controlled delivery of a non-steroidal anti-inflammatory drug, *Medical Engineering and Physics* 31 (2009) 1205–1213.
- [37] M.P. Ginebra, T. Traykova, J.A. Planell, Calcium phosphate cements as bone drug delivery systems: a review, *Journal of Controlled Release* 113 (2006) 102–110.
- [38] K. Kosmidis, P. Argyrak, P. Macheras, A reappraisal of drug release laws using Monte Carlo simulations: the prevalence of the Weibull function, *Pharmaceutical Research* 20 (2003) 988–995.
- [39] Y. Su, Q. Su, W. Liu, M. Lim, J.R. Venugopal, X. Mo, S. Ramakrishna, S. S. Al-Deyab, M. El-Newehy, Controlled release of bone morphogenetic protein 2 and dexamethasone loaded in core-shell PLLACL-collagen fibers for use in bone tissue engineering, *Acta Biomaterialia* 8 (2012) 763–771.
- [40] S. Hesarak, R. Nemati, Cephalixin-loaded injectable macroporous calcium phosphate bone cement, *Journal of Biomedical Materials Research B (Applied Biomaterials)* 89B (2009) 342–352.